

Effect of Time of Annealing on Gas Permeation through Coextruded Linear Low-Density Polyethylene (LLDPE) Films

Vicente Compañ,[†] Andreu Andrio,[†] María L. López,[†]
Cristina Alvarez,[‡] and Evaristo Riande^{*,‡}

Departamento de Física, Universitat Jaume I, 12080 Castellón, Spain, and Instituto de Ciencia y Tecnología de Polímeros, CSIC, 28006 Madrid, Spain

Received May 13, 1996; Revised Manuscript Received October 16, 1996[®]

ABSTRACT: The effect of annealing on the permeation of oxygen, nitrogen, and carbon dioxide through coextruded linear low-density polyethylene (LLDPE) films is studied. The results indicate that the permeability coefficient P of nitrogen does not show a definite dependence on the time of annealing, t_a , whereas for the other gases this parameter increases with t_a . The analysis of the variation of the diffusion coefficient of O_2 and N_2 with t_a indicates that D undergoes a sharp decrease from $t_a = 0$ to $t_a = 2$ h, but for larger times of annealing the diffusion parameter only undergoes a slight diminution; on the contrary, the diffusion coefficient of CO_2 gradually decreases with increasing t_a . The fact that annealing increases the solubility of the gases in the polymer films suggests that thermal treatments may favor the formation of microcavities or molecular packing defects in the crystalline amorphous interface that can accommodate individual site molecules without disturbing the natural dissolution process in the rubbery region of the polymer matrix. Finally, free volume theories are not sensitive enough to interpret the effect of annealing on the permeation characteristics of coextruded LLDPE films.

Introduction

Owing to the fact that gas diffusion in molecular barriers depends on the free volume available, permeation studies of gases through polymer membranes may afford a sensitive probe of polymer morphology. For example, all the steps involved in permeation processes through semicrystalline polymers, namely, sorption, diffusion, and desorption, take place in the amorphous region, the crystal entities acting as impermeable barriers. For systems of this kind in which the amorphous phase is in the rubbery state, permeation is largely reduced due to the fact that the crystalline entities force the penetrant to travel a longer path than in an amorphous rubbery material. Blocking factors arising from the narrowness of amorphous layers may hinder the passage of larger penetrants, thus affecting the permeation characteristics of semicrystalline membranes.^{1–5}

Studies on the temperature dependence of both the permeability and mechanical properties of coextruded linear low-density polyethylene (LLDPE) films suggest that melting and crystallization processes occurring above room temperature presumably affect the permeability and diffusion coefficients of gases through them.⁶ Further studies carried out on the permeation of oxygen and carbon dioxide through LLDPE films oriented by cold tensile drawing show that the permeability coefficients are rather insensitive to the drawing direction, though the values of these coefficients in the high-temperature region are significantly lower than those obtained through the undrawn films.⁷

Preliminary investigations carried out on gas permeation in coextruded LLDPE films indicate that annealing may have a strong effect on their permeability characteristics, giving rise to both a significant enhancement of the permeability and a slight decrease of the diffusion coefficient.⁸ Annealing may promote morphological changes in the crystalline amorphous interface

that may affect gas permeation through the films. Actually, coextruded LLDPE films are oriented in the extrusion direction, thus increasing the order in the crystalline–amorphous interface, and annealing may produce two effects in this interface: to favor coiled conformations, on the one hand, and to favor crystallite thickening, on the other hand. At first sight, these two phenomena will affect in opposite ways the permeation characteristics of the films.

In view of these facts, it was felt that we needed to investigate how both the permeability and the diffusion coefficients of gases through LLDPE films evolve with the time of annealing. These studies may be important not only on practical grounds, due to the extensive use of coextruded LLDPE films in the packaging industry, but also because they can shed light on how the morphological changes promoted by annealing may affect the solubility and diffusional characteristics of coextruded LLDPE films.

Experimental Part

Characteristics of LLDPE Films. The raw materials used in the preparation of the films utilized in this study are 1-octene-*co*-ethylene copolymers with roughly 8% mol content of the first comonomer. The films are made up of three layers, i.e. C(15 wt %)/A(70 wt %)/B(15 wt %). Layers A and C are Dowlex 2247 ($\rho = 0.917$ g cm⁻³), and layer B is Dowlex 2291 ($\rho = 0.912$ g cm⁻³). The films, supplied to us by Dario Manuli (Italy), were coextruded with three extruders C, A, and B at speeds of 88, 29, and 88 rpm, respectively, and the thicknesses of the layers comprising the films were 3.5, 16, and 3.5 μ m, respectively. The die-exit temperature was 270 °C, and the distances between the die and the chill roll (cooled with water at 20 °C) and between the die exit and the frost line were respectively 15 and 155 mm. Finally, the vacuum knife depression and the line speed were respectively 3.5 cmHg and 200 rpm.⁹

The thermal behavior of the films was determined with a Perkin-Elmer DSC-4 calorimeter at a heating rate of 8 °C min⁻¹. The thermogram of the films shows a small melting peak in the vicinity of 40 °C, which presumably corresponds to the fusion of very small crystalline entities followed by a wide melting endotherm that extends from 90 up to ca. 127 °C with the maximum of the peak located at ca. 122 °C. The degree of crystallinity of the films, determined from the

[†] Universitat Jaume I.

[‡] CSIC.

[®] Abstract published in *Advance ACS Abstracts*, May 1, 1997.

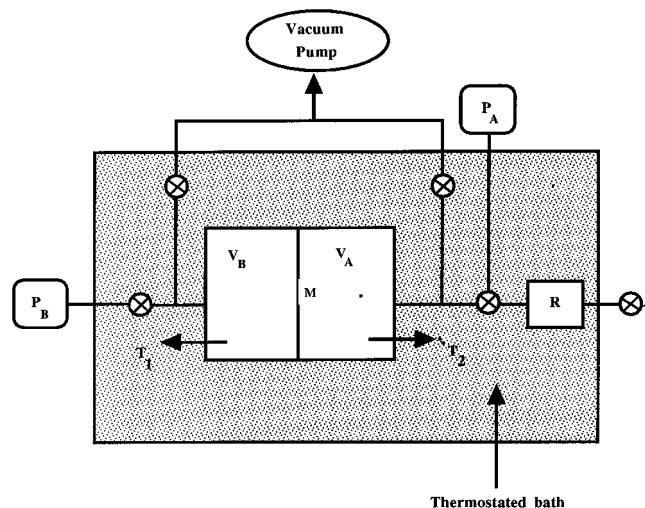


Figure 1. Scheme of the experimental device for the permeation measurements. T_1 and T_2 and P_A and P_B represent, respectively, temperature and pressure sensors. V_A and V_B are respectively the volumes of the high- and low-pressure chambers, while the symbols \otimes denote valves.

melting endotherm by assuming that the melting enthalpy is $960 \text{ cal (mol CH}_2\text{)}^{-1}$, was 0.30. The films exhibit birefringence as a consequence of their orientation in the extruding direction. The value Δn , measured with an Amplival Pol microscope at room temperature, was 1.40×10^{-3} .

Permeability Measurements. The experimental setup used in the permeability measurements is made up of two chambers separated by the film, as indicated in Figure 1. A reservoir with the diffusant gas at a pressure slightly above that of the measurement was placed in the thermostat containing the permeation cell. Once high vacuum throughout the experimental device immersed in the thermostat was made, the valve separating the reservoir from the cell was rapidly opened and the pressure in chamber A of volume V_A reached nearly instantaneously the pressure of $155 \pm 1 \text{ mmHg}$ at the temperature of the measurement. Opening of the valve was taken as the zero in the time scale. The evolution with time of the diffusants in the low-pressure chamber B was monitored by computer from a Leybold CM3 vacuum gauge provided with a capacitance sensor GDC 120. The permeation experiments were stopped once the pressure of diffusant in the low-pressure chamber was about 2% of the pressure in A. Each experiment was repeated three times, and the permeability coefficient was taken as the average of the values obtained. The experiments were performed over the temperature interval $20\text{--}80^\circ\text{C}$ and the temperature was kept within ± 0.1 deg of T .

Experimental Results

Under conditions of steady state permeation, the permeability coefficient P can be obtained by means of the following expression

$$P = \frac{273}{76} \left(\frac{V_B I}{A T p_0} \right) \left(\frac{dp_i(t)}{dt} \right) \quad (1)$$

where A and I are respectively the effective area and the thickness of the film, T is the temperature of the measurement in K, and p_i represents the evolution of the downstream pressure. P is usually expressed in barrers [$=10^{-10} \text{ (cm}^3 \text{ (STP) cm)/(cm}^2 \text{ s cmHg)}$].

In nonsteady state conditions, gas permeation in films is described by the second law of Fick, as follows

$$\frac{\partial C}{\partial t} = D \frac{\partial^2 C}{\partial x^2} \quad (2)$$

The solution of this equation using the boundary conditions^{10,11}

$$C(x=0, t < 0) = 0; \quad C(x=I, t < 0) = 0 \quad (3)$$

$$C(x=0, t \geq 0) = C_0; \quad C(x=I, t \geq 0) \cong 0 \quad (4)$$

permits us to obtain the expression

$$Q(t) = \frac{DC_0}{I} \left(t - \frac{l^2}{6D} \right) \quad (5)$$

where $Q(t)$ represents the amount of gas per unit of area that up to time t would flow through the membrane in steady state conditions. Then the diffusion coefficient can be obtained from the intercept with the time axis, θ , of the plot p_i against t , as suggested by Barrer.¹² Accordingly,

$$D = \frac{l^2}{6\theta} \quad (6)$$

Significant errors may be involved in the determination of D by the lag method, arising, in most cases, from the small thickness of the films ($\approx 25 \mu\text{m}$). Actually, the smaller the thickness, the lower is θ and, consequently, the larger is the uncertainty of the value of D obtained by this method. Moreover, since D depends on l^2 , the uncertainty in the measurement of l for thin films may also give rise to a significant error in the value of D . Actually, the relative error involved in the determination of the diffusion coefficient of oxygen through LLDPE films is given by

$$\text{relative error} = 100 \times \left[\frac{2\epsilon(l)}{6\theta} + \frac{l^2 \epsilon(\theta)}{6\theta^2} \right] / D \quad (7)$$

where $\epsilon(l)$ and $\epsilon(\theta)$ are, respectively, the errors involved in the measurements of the thickness and lag time. It should be pointed out that $\epsilon(\theta)$ was obtained from three consecutive permeability measurements carried out on the films at the temperatures of interest. Let us now determine the error involved in the determination of D for oxygen, at 35°C , in a sample annealed for 2 h. In this case, $l = 23 \pm 1 \mu\text{m}$ and $\theta = 5.6 \pm 1.4 \text{ s}$ so that the relative error is 33%. From the same type of experiment in a nonannealed film one obtains $\theta = 2 \pm 2 \text{ s}$, at the same temperature, and the relative error is ca. 100%.

In view of the significant errors involved in the determination of D , arising from the extreme thickness of the films, the permeation measurements were performed in membranes made up of three films firmly stuck together with a rolling cylinder at room temperature. Boundary effects at the interface between films were not detected, as indicated by the fact that the flow through membranes containing different numbers of films scales with the reciprocal of the membrane thickness (Figure 2). As will be discussed below, annealing decreases the diffusion coefficient and, consequently, the relative error of the values of D obtained by the lag time method decreases as the time of annealing increases. For illustrative purposes, the relative errors estimated in the determination of the diffusion coefficient at 25 and 55°C are given in Table 1. It can be seen that, even in the most unfavorable cases, the error in D is lower than 15% in the interval of temperature indicated.

The effect of annealing on the permeant characteristics of coextruded LLDPE films was investigated by studying the temperature dependence of the perme-

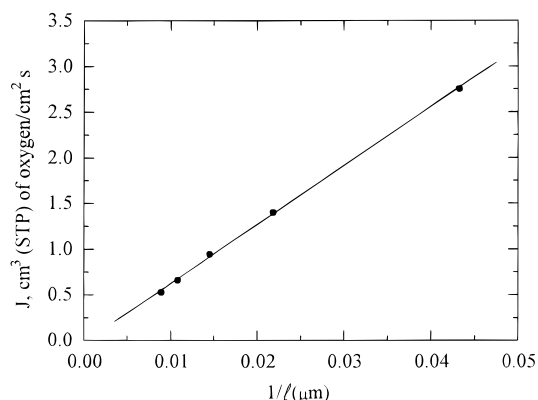


Figure 2. Plot showing the flux of oxygen as a function of the reciprocal of the thickness of membranes made up of LLDPE films firmly stuck together.

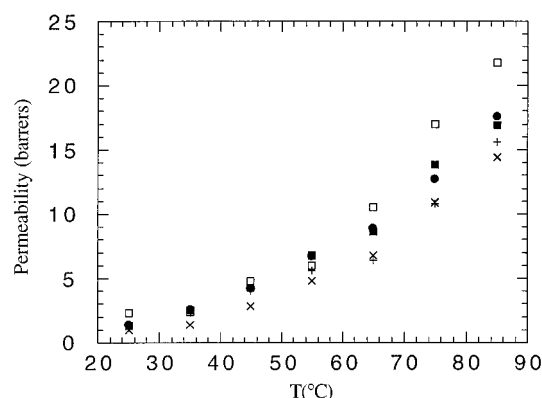


Figure 3. Temperature dependence of the permeability coefficient of nitrogen through LLDPE membranes previously annealed at 85 °C for (■) 0, (□) 2, (×) 6, (+) 12, and (●) 24 h.

Table 1. Illustrative Examples of the Relative Errors Estimated in the Determination of the Diffusion Coefficients of Nitrogen, Oxygen, and Carbon Dioxide in LLDPE Membranes

<i>T</i> , °C	time of annealing, h	gas	lag time, s	$10^7 D$, cm ² s ⁻¹	rel error, %
25	0	N ₂	14.4 ± 1.5	5.5	13.0
25	24	N ₂	88.2 ± 2.8	0.9	5.4
55	0	N ₂	12.8 ± 1.1	6.2	11.3
55	24	N ₂	41.8 ± 2.3	1.9	7.9
25	0	O ₂	17.6 ± 1.4	4.5	10.7
25	24	O ₂	72.1 ± 3.1	1.1	6.4
55	0	O ₂	12.6 ± 1.4	6.3	13.8
55	24	O ₂	34.5 ± 2.1	2.3	8.7
25	0	CO ₂	17.6 ± 1.5	4.5	11.3
25	24	CO ₂	52.9 ± 2.8	1.5	7.3
55	0	CO ₂	9.8 ± 1.0	8.1	13.0
55	24	CO ₂	24.0 ± 1.9	3.3	10.6

ability, diffusion, and solubility coefficients of some representative gases in membranes annealed at 85 °C for 2, 6, 12, and 24 h. For comparative purposes, the temperature dependence of these parameters was also investigated in not annealed membranes. The permeation results are summarized in Figures 3–5 where the changes occurring on the values of the permeability coefficient of nitrogen, oxygen, and carbon dioxide with temperature are shown. Although in all the cases the permeability coefficient increases with temperature, the effect of annealing on this parameter depends on the diffusant. Thus, whereas the permeability coefficient of N₂ does not show a definite dependence on the thermal treatment, the values of *P*, for the other gases, seem to increase with the time of annealing, *t_a*. For example, the values of *P* for O₂ at 25 and 85 °C in the

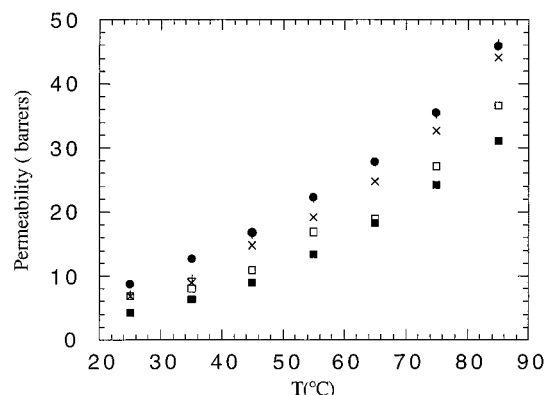


Figure 4. Variation of the permeability coefficient of oxygen with temperature through LLDPE membranes previously annealed at 85 °C for (■) 0, (□) 2, (×) 6, (+) 12, and (●) 24 h.

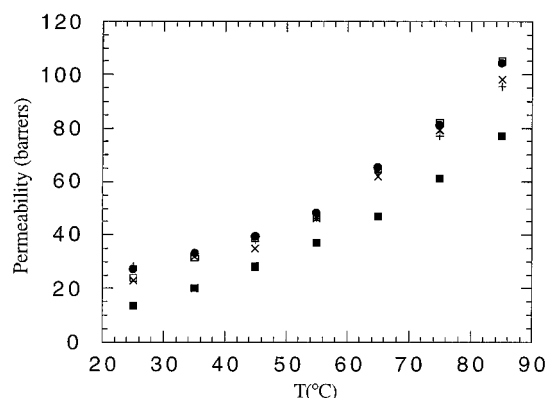


Figure 5. Temperature dependence of the permeability coefficient of carbon dioxide through LLDPE membranes previously annealed at 85 °C for (■) 0, (□) 2, (×) 6, (+) 12, and (●) 24 h.

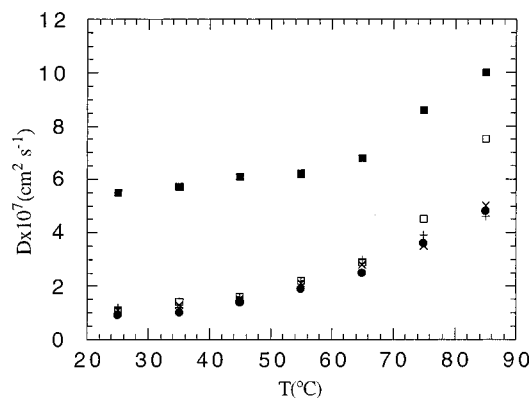


Figure 6. Temperature dependence of the diffusion coefficient of nitrogen through LLDPE membranes annealed at 85 °C for (■) 0, (□) 2, (×) 6, (+) 12, and (●) 24 h.

not annealed membrane are 4 and 31 barrers, respectively, and these values rise to 9 and 46 barrers, respectively, in the membranes annealed at 85 °C for 24 h. On the other hand, although the permeability coefficient of CO₂ in the not annealed membranes is significantly lower than that in the annealed ones, the values of this parameter do not show a definite dependence on the annealing time for *t_a* > 2 h.

Figures 6–8 show respectively the effect of annealing on the diffusion coefficients of nitrogen, oxygen, and carbon dioxide. It can be seen that the diffusion coefficient of CO₂ at each temperature gradually decreases with *t_a*, the values of 10⁷*D* at 85 °C changing from 14.5 cm² s⁻¹ for *t_a* = 0 to 6 cm² s⁻¹ for *t_a* = 24 h; at

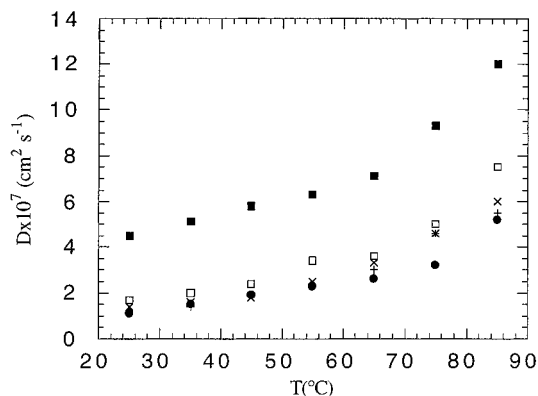


Figure 7. Temperature dependence of the diffusion coefficient of oxygen through LLDPE membranes annealed at 85 °C for (■) 0, (□) 2, (×) 6, (+) 12, and (●) 24 h.

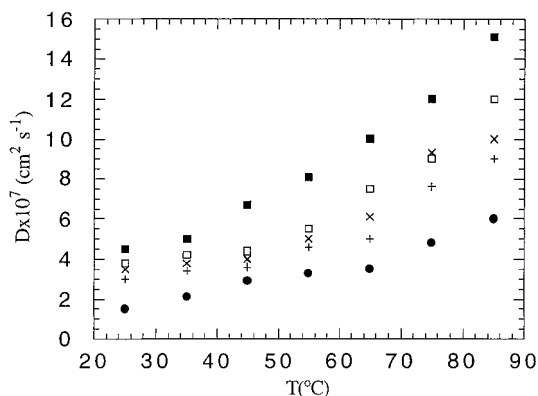


Figure 8. Variation of the diffusion coefficient of carbon dioxide with temperature in LLDPE membranes previously annealed at 85 °C for (■) 0, (□) 2, (×) 6, (+) 12, and (●) 24 h.

25 °C, these changes are only from 4.25 to 1.75 $\text{cm}^2 \text{ s}^{-1}$, respectively. The values of the diffusion coefficient of oxygen undergo a rather sharp decrease between $t_a = 0$ and 2 h, the values of D in the former case being nearly 2 times larger than those in the latter. As t_a increases between 2 and 24 h, a gradual and moderate decrease in the values of D at each temperature of interest occurs. As far as the dependence of the diffusion coefficient of nitrogen on t_a is concerned, this parameter behaves in a way similar to that observed in oxygen.

Discussion

As usual,¹³ the permeability coefficients of the gases used in this study increase in the following order: $P(\text{CO}_2) > P(\text{O}_2) > P(\text{N}_2)$. Similar trends also hold for the diffusion coefficient at most temperatures. On the other hand, the fact that the thermal treatment tends both to increase the permeability coefficient and to decrease the diffusion coefficient suggests that annealing changes, in a significant way, the values of the apparent solubility coefficient ($S = P/D$) of the gases in the membranes. The curves depicting the dependence of the apparent solubility coefficient on both annealing time and temperature for nitrogen, oxygen, and carbon dioxide, shown in Figures 9–11, respectively, exhibit the same pattern. In all the cases the solubility coefficient gradually increases with the annealing time. For example, the value of S for O_2 in $10^{-3} \text{ (cm}^3 \text{ of gas/cm}^3 \text{ of polymer cmHg)}$ goes up from 1 to 8, at 25 °C, when t_a increases from 0 to 24 h. These changes in the apparent solubility coefficient, at the same temperatures, are from 3 to 18 and from 0.2 to 1.5, in the same units, for CO_2

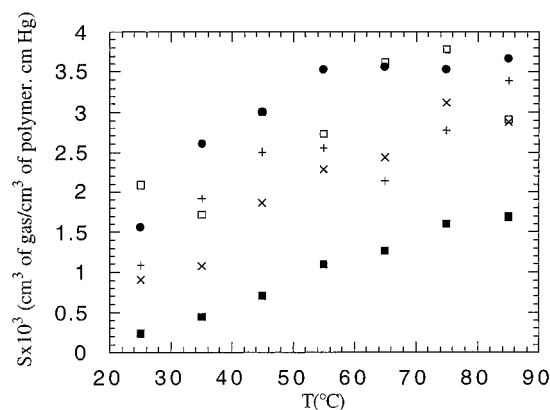


Figure 9. Temperature dependence of the solubility coefficient of nitrogen in LLDPE membranes annealed at 85 °C for (■) 0, (□) 2, (×) 6, (+) 12, and (●) 24 h.

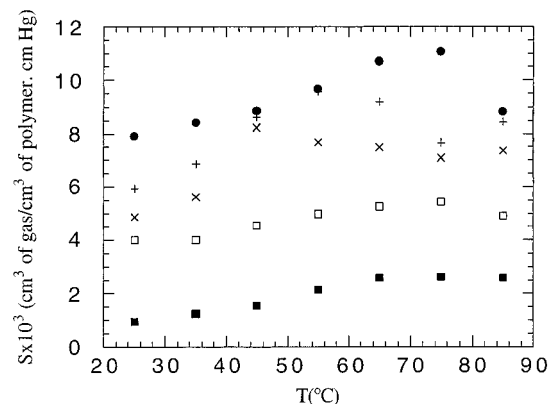


Figure 10. Plot showing the variation of the solubility coefficient of oxygen in LLDPE membranes annealed at 85 °C for (■) 0, (□) 2, (×) 6, (+) 12, and (●) 24 h.

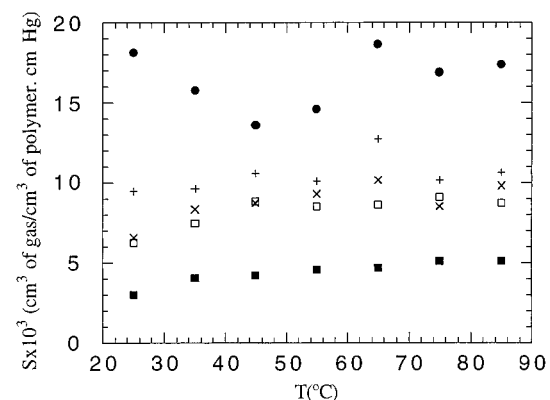


Figure 11. Values of the solubility coefficient against temperature for carbon dioxide in membranes annealed at 85 °C for (■) 0, (□) 2, (×) 6, (+) 12, and (●) 24 h.

and N_2 , respectively. It is noteworthy that the value of the solubility coefficient either remains constant or undergoes a slight increase with increasing temperature. Moreover, as expected, $S(\text{CO}_2) > S(\text{O}_2) > S(\text{N}_2)$. Because gas solubility preferentially occurs in the amorphous regions of semicrystalline polymers, the increase in solubility with annealing suggests at first sight that the overall effect of the heat treatment may be to increase the formation of coiled regions. Obviously, this can be accomplished by melting of low-size crystalline entities and also by coiling oriented parts of the crystalline amorphous interface.

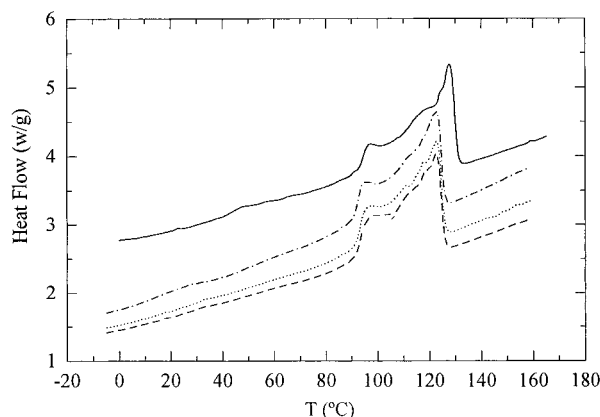


Figure 12. Thermal behavior of coextruded LLDPE films annealed at 85 °C for (---) 0, (— · —) 2, (···) 4 and (—) 6 h.

The possible changes in the morphology of the films which could arise from annealing were qualitatively investigated by DSC calorimetry and birefringence. A close inspection of the thermograms obtained for different annealing times, represented in Figure 12, shows that a weak and blurred peak appearing in the vicinity of 40 °C in the not annealed membrane is absent in the annealed ones. This peak, characteristic of LLDPE films, presumably reflects the melting of very small crystalline entities. Moreover, the shape and intensity of the melting peak centered in the vicinity of 120 °C do not show a noticeable dependence on the annealing time. Annealing also does not affect, in a significant way, the birefringence of the films. Thus the values of $10^3 \Delta n$ at room temperature amount to 1.40 ± 0.03 , 1.58 ± 0.03 , 1.64 ± 0.06 , 1.58 ± 0.06 , 1.46 ± 0.11 , and 1.55 ± 0.09 , respectively, for the membranes whose annealing times are $t_a = 0, 2, 4, 6, 12$, and 24 h. The fact that annealing does not seem to give rise to significant differences either in the thermal behavior or in the birefringence suggests that the increase observed in the permeability of O_2 and CO_2 through the annealed membranes may be the overall effect of morphological changes arising from the melting of the smallest crystalline entities and from two apparently opposite processes: coiling of the ordered interfaces and crystallites thickening¹⁴ at the expense of the crystalline–amorphous interface.

Gas diffusion through isotropic barriers is an activated process that obeys Arrhenius behavior. In general, the Arrhenius plots for the diffusion coefficient in semicrystalline polymers fit rather poorly to straight lines, as reflected by the low correlation coefficients obtained, which lie in the range 0.90–0.95. This is a consequence of both the lack of isotropy and the morphological changes occurring with temperature in the films. In any case the activation energy associated with the transport of oxygen and nitrogen in annealed membranes seems to be somewhat higher than that involved in the diffusive transport of these gases in the not annealed ones. For example, the apparent values of the activation energy for the diffusive transport of oxygen in membranes annealed for 0 and 2 h are, respectively, 3.3 ($r = 0.93$) and 5.0 ($r = 0.95$) kcal mol⁻¹; these changes seem to be even somewhat higher for nitrogen and negligible for carbon dioxide. The diffusion coefficient reflects the speed with which the gas permeation reaches steady state conditions and, consequently, depends on the size of the permeant and the structure of the matrix through which diffusion occurs. Michaels and Parker² assume that the apparent diffu-

sion coefficient through semicrystalline membranes is given by

$$D = \frac{D^*}{\tau\beta} \quad (8)$$

where D^* is the diffusion coefficient for the completely amorphous polymer, τ accounts for the tortuosity of the diffusive path caused by the crystalline entities, and β is mainly related to the lack of mobility in the amorphous regions close to the anchoring points in the crystals.¹⁵ According to the model, the fact that the activation energy of the apparent diffusion coefficient through the not annealed membranes is somewhat lower than that in the annealed ones suggests that annealing may produce morphological changes that cause additional obstruction to the diffusion. Annealing processes may then favor the formation of microcavities (molecular packing defects) in the crystalline–amorphous interface that can accommodate individual site molecules without disturbing the normal dissolution process in the rubbery region of the polymer matrix. According to this interpretation, annealing may cause crystallite thickening that hinders gas permeation but also may provide packing defects in the crystalline amorphous interface that can act as sorption sites for the permeants, thus increasing the solubility coefficient.

Following Stern and co-workers,^{16–18} the diffusion of small molecules through semicrystalline polymers can be expressed in terms of Fujita's free volume¹⁹ model by means of the expression

$$D = RTA_d \exp\left(\frac{B_d}{\phi_a v_f}\right) \quad (9)$$

where ϕ_a is the volume fraction of amorphous polymer, v_f is the fractional free volume, and A_d and B_d depend on penetrant molecular size. The last parameter is assumed to be a constant close to unity, though more rigorous treatments suggest that its value depends on the size of the polymer unit jumping and the minimum size of hole required for a diffusive jump to occur. The fractional free volume, which depends on the pressure in the high-pressure chamber, temperature, and the penetrant concentration as free volume, can be written as¹⁶

$$v_f(T) = v_{fs}(T_s, p_s) + \alpha(T - T_s) - \beta(p - p_s) + \gamma v \quad (10)$$

where $v_{fs}(T_s, p_s)$ is the fractional free volume at some reference temperature T_s and pressure p_s and α ($=(\partial v_f / \partial T)_s$), β ($=(\partial v_f / \partial p)_s$), and γ ($=(\partial v_f / \partial v)_s$) are coefficients which define the effectiveness of the penetrant as a plastizicer. At low pressures, like those used in this work, eq 10 is approximately given by

$$v_f(T) = v_{fs}(T_s) + \alpha(T - T_s) \quad (11)$$

A rather good approximation for the fractional free volume of LLDPE can be obtained from the following relationship

$$v_f(T) = \frac{v_l(T) - v_c(T)}{v_l(T)} \quad (12)$$

where v_l and v_c are respectively the specific volume of the amorphous and crystalline phases of LLDPE. In the evaluation of the fractional free volume, use was made of the temperature dependence of v_l and v_c

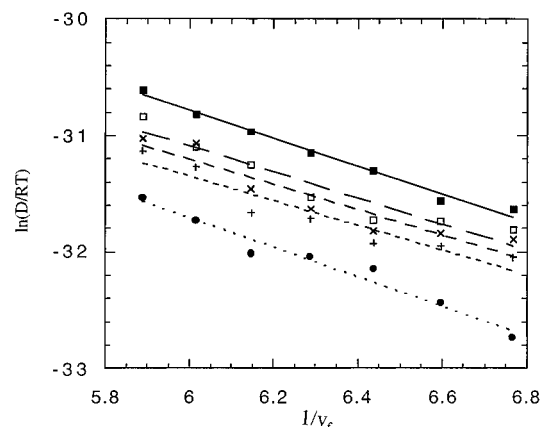


Figure 13. Dependence of the diffusion coefficient on the free volume for carbon dioxide in membranes annealed at 85 °C for (■) 0, (□) 2, (×) 6, (+) 12, and (●) 24 h.

Table 2. Influence of Annealing on the Free Volume Parameters of Coextruded LLDPE Films for N₂, O₂, and CO₂^a

annealing time, h	gas	10 ¹¹ A _d	B _d
0	N ₂	(0.04)	0.44
2		(136)	0.84
6		12.0	1.20
12		11.2	1.49
24		52.1	1.78
0	O ₂	0.5	0.95
2		8.9	0.97
6		13.1	0.97
12		20.7	0.99
24		4.8	0.97
0	CO ₂	5.8	1.20
2		2.6	1.12
6		1.9	1.09
12		1.4	1.06
24		3.0	1.26

^a A_d has units of (m² g mol)/(s J) and B_d is dimensionless.

reported by Chiang and Flory²⁰ for polyethylene, given by

$$v_f(T) = 1.152 + 8.8 \times 10^{-4}(T - 273.15) \quad (13)$$

$$v_c(T) = 0.993 + 3.0 \times 10^{-4}(T - 273.15) \quad (14)$$

With few exceptions, the plots of $\ln(D/RT)$ against $1/v_f$ fit fairly well to straight lines, as indicated in Figure 13 where, as an example, the data corresponding to the diffusion of CO₂ are shown. The values of A_d and B_d for N₂, O₂, and CO₂, obtained respectively from the slopes and intercepts in the ordinate axis of the corresponding straight lines, are listed in Table 2. It should be pointed out that the values thus obtained for A_d involve some uncertainty owing to the fact that it is necessary to extrapolate to $v_f - 1 = 0$ from rather limited values of v_f . Stern and co-workers¹⁷ performed a thorough study on the permeation of gases through polyethylene films, finding that the values of A_d and B_d for CO₂ are 5.4×10^{-11} (m² g mol)/(s J) and 0.40,

respectively. Whereas in these results the value of A_d compares satisfactorily with that given for CO₂ in not annealed LLDPE membranes, the value of B_d is nearly half of that found in these membranes. The results in Table 2 do not show a definite dependence of B_d on annealing time, except in the case of N₂ where this parameter seems to increase with t_a . The fact that free volume parameters for CO₂ and O₂ do not show a definite variation with annealing time suggests that the changes that annealing may produce in the free volume are not important enough to affect in a decisive way the gas diffusion through LLDPE films.

The results discussed above suggest that gas permeation through LLDPE films is a rather complex process in which solubility seems to play a leading role. Morphological changes occurring in the films during annealing seem to favor the formation of molecular packing defects which presumably act as sorption sites for the permeant. Consequently, to get a better understanding of the diffusant characteristics of LLDPE films would require us to carry out further studies by both X-ray and Raman spectroscopy to determine the effect of annealing on the distribution of crystallites in these films.

Acknowledgment. This work was supported by the DGICYT through Grant PB95-0134-C02.

References and Notes

- (1) Michaels, A. S.; Bixler, H. J. *J. Polym. Sci.* **1961**, *50*, 393.
- (2) Michaels, A. S.; Parker, R. B., Jr. *J. Polym. Sci.* **1959**, *41*, 33.
- (3) Myers, A. W.; Rogers, C. E.; Stannett, V.; Szwarc, M. *Tappi* **1958**, *41*, 716.
- (4) Capaccio, G.; Gibson, A. G.; Ward, I. M. In *Ultra-High Modulus Polymers*; Ciferri, A., Ward, I. M., Eds., Applied Science: London, 1979; Chapter I.
- (5) Holden, P. S.; Orchard, G. A. J.; Ward, I. M. *J. Polym. Sci., Polym. Phys. Ed.* **1985**, *23*, 709.
- (6) Compañ, V.; Ribes, A.; Díaz-Calleja, R.; Riande, E. *Polymer* **1995**, *36*, 323.
- (7) Compañ, V.; Ribes, A.; Díaz-Calleja, R.; Riande, E. *Polymer* **1996**, *37*, 2243.
- (8) Compañ, V.; Andrio, A.; López, M. L.; Riande, E. *Polymer* **1996**, *37*, 5831.
- (9) *Quality Enhancement and Process Availability in LLDPE Stretch Film by Multisensors and Computirized System*; Forni, C., Coordinator; Brite-Euram-BE Project 4104; Brussels, 1995.
- (10) Carslaw, H. S.; Haeger, L. *Conduction of Heat in Solids*; Oxford University Press: Oxford, U.K., 1959; p 213.
- (11) Crank, J. *The Mathematics of Diffusion*, 2nd ed.; Clarendon: Oxford, U.K., 1975.
- (12) Barrer, R. M. *Trans. Faraday Soc.* **1939**, *35*, 628.
- (13) Glatz, F. P.; Mülhaupt, R. *J. Membr. Sci.* **1991**, *90*, 151.
- (14) Benavente, R.; Pereña, J. M.; Bello, A.; Aguilar, C.; Martinez, M. C. *J. Mater. Sci.* **1990**, *25*, 4162.
- (15) Michaels, A. S.; Bixler, H. J.; Fein, H. L. *J. Appl. Phys.* **1964**, *35*, 3165.
- (16) Stern, S. A.; Fang, S.-M.; Frisch, H. L. *J. Polym. Sci.; Part 2* **1972**, *10*, 201.
- (17) Stern, S. A.; Kulkarni, S. S.; Frisch, H. L. *J. Polym. Sci., Polym. Phys. Ed.* **1983**, *21*, 467.
- (18) Stern, S. A.; Sampat, S. R.; Kulkarni, S. S. *J. Polym. Sci., Polym. Phys. Ed.* **1986**, *24*, 2149.
- (19) Fujita, H. *Fortschr. Hochpolym. Forsch.* **1967**, *3*, 1.
- (20) Chiang, R.; Flory, P. J. *J. Am. Chem. Soc.* **1961**, *83*, 2857.

MA960691C